Desalination and Water Treatment
www.deswater.com

doi: 10.5004/dwt.2020.25803

192 (2020) 431–436
July

Temperature dependence modeling of reverse osmosis

G. Lakner[a,*], J. Lakner[a], G. Racz[a], M. Kłos[b]

[a]*Hidrofilt Kft, Magyar utca 191, 8800 Nagykanizsa, Hungary, Tel. +36 30 579 7930; Fax: +93 536 500; emails: lakner.g@hidrofilt.hu (G. Lakner), lakner.jozsef@amk.uni-obuda.hu (J. Lakner), racz.g@hidrofilt.hu (G. Racz)*
[b]*Faculty of Energy and Environmental Engineering, Institute of Water and Wastewater Engineering, The Silesian University of Technology, Konarskiego 18, 44-100 Gliwice, Poland, email: marcin.klos@polsl.pl (M. Kłos)*

Received 18 October 2019; Accepted 6 March 2020

ABSTRACT

Osmosis is the natural flow of a solvent through a semi-permeable membrane from a less concentrated solution to a more concentrated one. This is driven by the osmotic pressure difference. If opposing external pressure exceeding the osmotic pressure is used, the solvent will flow from the more concentrated solution toward the less concentrated one. This is reverse osmosis, whose main characteristic, as for any mass transfer process, is the mass transfer coefficient. This mass transfer coefficient is dependent on temperature, and there are several empirical correlations for it. In this study, an Arrhenius-type correlation is deduced for the temperature dependence of the mass transfer coefficient based on the Poiseuille law, which appropriately describes the dependence of both the solvent (water) flow through the membrane and the salt rejection – as the most important characteristic of the system – on the handling temperature. The activation energy, E_a = 25 kJ mol^{-1}, determined on the basis of the Arrhenius correlation, is equal to that of the transmembrane processes and can be linked to the membrane structure. The controlling of the model was certified by reverse osmotic desalination of seawater based on independent measurements from the literature.

Keywords: Reverse osmosis; Flux; Mass transfer coefficient; Temperature dependence; Arrhenius equation

1. Introduction, reverse osmosis

Osmosis is the natural flow of a solvent through a semi-permeable membrane from a less concentrated solution to a more concentrated one. The driving force is the osmotic pressure difference, which is the function of the solvent, the type of dissolved material, and the concentration. When the developed hydrostatic pressure is exactly the same as the osmotic pressure, the result is osmotic equilibrium, when the net mass transfer through the membrane is zero. If we apply over-pressure on the side of the more concentrated solution, the direction of the natural osmosis is reversed.

The solvent will flow from the more concentrated solution toward the less concentrated one. So this process, reverse osmosis, is the reversal of natural osmosis due to hydrostatic pressure. In the case of reverse osmosis, the driving force is the hydrostatic pressure difference, and the mass transfer mechanism is molecular diffusion [1]. In the case of reverse osmosis, as with all cross-flows, there is a concentration difference in the solution, which is perpendicular to the membrane wall [2]. This concentration polarization further modifies the value of the osmotic pressure, and through this, the concentration dependence of the flux [3].

The osmotic flow is proportional to the difference between the overpressure and the osmotic pressure difference. The proportionality factor is the mass transfer coefficient (permeability) [4]. According to the van't Hoff law, the

* Corresponding author.

Presented at PERMEA 2019, 26–29 August 2019, Budapest, Hungary

osmotic flow is, linearly, dependent on the salt concentration [5], on temperature [6] and, finally, on the membrane material [7].

A predictive model based on the solution–diffusion theory is proposed for commercial reverse osmosis modules [8]. Using experimental data, it is shown that the permeate water and salt concentrate increase with temperature based loosely on Arrhenius-type equations [9,10]. The actual temperature dependence is exponential, which is usually described by an empirical formula [11], which can originate from the temperature dependence of the mass transfer coefficient [12].

In this study, an Arrhenius-type correlation is deduced for the temperature dependence of the mass transfer coefficient based on the Poiseuille-law, which appropriately describes the dependence of both the solvent (water) flow through the membrane and the salt rejection – as the most important characteristic of the system – on the handling temperature. The controlling of the model was certified by reverse osmotic desalination of seawater based on independent measurements from literature.

2. Modeling temperature dependence

2.1. Diffusion model, water flux

In the case of reverse osmosis, permeate flows depend on the diffusion mass transport, both for salt and water. The water flux is created by the transmembrane $\left(\Delta p = p_f - p_p\right)$ and osmotic pressure difference $\left(\Delta\pi = \pi_f - \pi_p\right)$ between the feed (*f*) and permeate (*p*) side, as the function of the concentration difference, namely:

$$J_w = K_w(\Delta p - \Delta\pi) \tag{1}$$

where K_w can be defined as the mass transfer coefficient for the water as permeability [4]. The flux is linearly dependent on the transmembrane pressure; if $\Delta p < \Delta\pi$, water flows toward the concentrated salt solution (normal osmosis), if $\Delta p > \Delta\pi$, it flows in the opposite direction (reverse osmosis). If $\Delta p = \Delta\pi$ there is equilibrium, and so $J_w = 0$.

Besides water, salt also flows through the membrane. The salt flux in line with Eq. (1), in the case of reverse osmosis, can be described as usual [13] with the following equation:

$$J_s = K_s(C_f - C_p) \cong K_s C_f \tag{2}$$

where K_s is the mass transfer coefficient for salt (permeate), C_f is the feed side, and C_p is the permeate side concentration. Since $C_p << C_f$, $C_p = 0$ can be assumed in Eq. (2).

2.2. Salt rejection

There are several ways to measure the selectivity of the membrane. Here, we are going to use salt rejection [13], which is as follows:

$$R = \left[1 - \frac{C_p}{C_f}\right] \times 100\ (\%) \tag{3}$$

Since the salt flux arriving at the membrane is $J_s = J_w \cdot C_f$, [17] and using Eq. (2), the salt rejection from Eq. (3) can be finally expressed in the form of the following equation [17]:

$$R = \left[1 - \frac{K_s C_f}{J_w}\right] \times 100(\%) \tag{4}$$

2.3. Formal model of the water flux temperature dependence

Temperature plays a central role in the process of reverse osmosis. The correlation between permeate flux and temperature can be described as follows: Let us choose a reference temperature, T_0. T and T_0 are the fluxes associated with the temperatures:

$$\mathrm{TFC} = \frac{J_w}{J_{w,0}} \tag{5}$$

The ratio of J_w and $J_{w,0}$ is the correction factor of temperature, which can be expressed in the following empirical form:

$$\mathrm{TFC} = e^{\beta\left(\frac{1}{T_0} - \frac{1}{T}\right)} \tag{6}$$

where $\beta > 0$ (K) is a temperature constant for the given membrane material [11]. Eq. (6) can be transcribed into the following form:

$$\mathrm{TFC} = e^{\beta\frac{T - T_0}{T_0 T}} = a \cdot e^{-\frac{\beta}{T}} \tag{7}$$

where $a = e^{\frac{\beta}{T_0}}$. According to this, using Eq. (5) the permeate flux is the following:

$$J_w = a J_{w,0} e^{-\frac{\beta}{T}} \tag{8}$$

which rises exponentially with the temperature.

2.4. Transmembrane transition model, Arrhenius-type temperature dependence

The main flow resulting from the Δp pressure difference across a membrane with cylindrical pores is described by the Poiseuille-law for the individual pores [13]:

$$j_w = \frac{\pi\delta^4}{128\eta\lambda} \cdot \Delta p \tag{9}$$

where $\delta \geq 0$ is the pore diameter, λ is the length, and η is the viscosity of the liquid (water). The flux is the sum of the main flows through the pores, related to a unit of surface:

$$J_w = n \cdot j_w = n \cdot \frac{\pi\delta^4}{128\eta\lambda} \cdot \Delta p \tag{10}$$

where n is now the number of pores per unit of membrane surface as follows:

$$n = \varepsilon \frac{4}{\pi\delta^2} \tag{11}$$

which is directly proportional to the porosity ε and inversely to the cross section of pore, $\delta^2\pi/4$.

Finally, the flux through the membrane, by comparing Eqs. (10) and (11), will be:

$$J_w = \frac{\varepsilon\delta^2}{32\eta\lambda} \times \Delta p \tag{12}$$

Comparing Eq. (1) (in the case $\Delta\pi \to 0$) with Eq. (12):

$$K_w = \frac{\varepsilon\delta^2}{32\lambda}\frac{1}{\eta} \tag{13}$$

where the K_w mass transfer coefficient for the water is inversely proportional to the viscosity of the liquid, η, where the proportionality factor consists of the membrane characteristics.

The temperature dependence of the (water) viscosity is determined by the Arrhenius-type temperature dependence that can be defined based on Frenkel's hole theory [14]:

$$\eta = \eta_0 e^{\frac{E_\eta}{R_g T}} \tag{14}$$

where, in the case of water, $\eta_0 = 0.0015$ is the pre-exponential coefficient and $E_\eta = 16$ kJ mol^{-1} is [15].

According to this, Eq. (13) mass transfer coefficient for the water is an Arrhenius-type correlation, that is:

$$K_w = K_{w,0} e^{-\frac{Ea,w}{R_g T}} \tag{15}$$

with the pre-exponential coefficient, $K_{w,0} = \frac{\varepsilon\delta^2}{32\eta_0}$, and activation energy $E_{a,w}$, according to the model, $E_{a,w} = E_\eta$.

The activation energy is a potential barrier through which only molecules with an energy exceeding their height can pass [16]. This extra energy is provided by thermal fluctuation, as a result of which the mass transfer coefficient is dependent on temperature according to Eq. (15).

2.5. Osmotic pressure

The osmotic pressure difference in Eq. (1), Δπ, can be described for small concentrations (ideal solution) on the basis of the van't Hoff law [6]:

$$\Delta\pi = \alpha R_g T C_f \tag{16}$$

where $\alpha = K_a \cdot \nu, K_a$, K_a is the dissociation constant, and ν is the dissociation number (in the case of NaCl, $K_\alpha = 1$, $\nu = 2$, i.e., $\alpha = 2$) [16,17].

For greater concentrations (real solution), the osmotic pressure will be:

$$\Delta\pi = \alpha R_g T f_0 C_f = \alpha R_g T f_0 C_f \tag{17}$$

where the f_0 is the osmotic constant ($f_0 = 1 - 0.137 C_f^{0.5}$m%, NaCl) [16,17] and $f_0 C_f$ equivalent concentration means the concentration value that would be the value associated with the identical osmotic pressure in the case of an ideal solution [17].

During the reverse osmotic process, a concentration at the membrane wall is $C_m > C_f$ by polarization, therefore the osmotic pressure will be proportional to the salt concentration at the membrane wall C_m. This latter depends on the transmembrane pressure, that is $C_m = (1 + q\Delta p) C_f$, where q is a ratio ($q = 0.0022$) [17]. Accordingly, in the case of polarization, the transmembrane pressure depends on the transmembrane pressure over and above salt concentration:

$$\Delta\pi \cong \alpha R_g T (1 + q\Delta p) f_0 C_f \tag{18}$$

2.6. Water flux temperature dependence

The water flux has an Arrhenius-type correlation by mass transfer coefficient of Eq. (15), K_w, which, comparing Eqs. (1) and (18) and rearranging it as:

$$K_w = \frac{J_w}{\Delta p - \alpha R_g T (1 + q\Delta p) f_0 C_f} \tag{19}$$

Using Eq. (15) and considering the logarithm of both sides:

$$\ln K_w = \ln K_{w,0} - \frac{E_{a,w}}{R_g}\frac{1}{T} \tag{20}$$

A line correlation can be obtained, the slope of which is proportional to the Eq. (15) mass transfer coefficient activation energy of the water flux $E_{a,w}$, while its axial section is the logarithm of the pre-exponential coefficient.

2.7. Temperature dependence of salt rejection

The mass transfer coefficient for the salt, similarly to Eq. (15), can also be formulated as an Arrhenius-type correlation, namely:

$$K_s = K_{s,0} e^{-\frac{E_{a,s}}{R_g T}} \tag{21}$$

where $E_{a,s}$ is the activation energy of the salt transfer process, and $K_{s,0}$ is the associated pre-exponential coefficient [16].

The salt transfer coefficient from Eq. (4) will be:

$$K_s = \frac{100 - R}{100 C_f} J_w \tag{22}$$

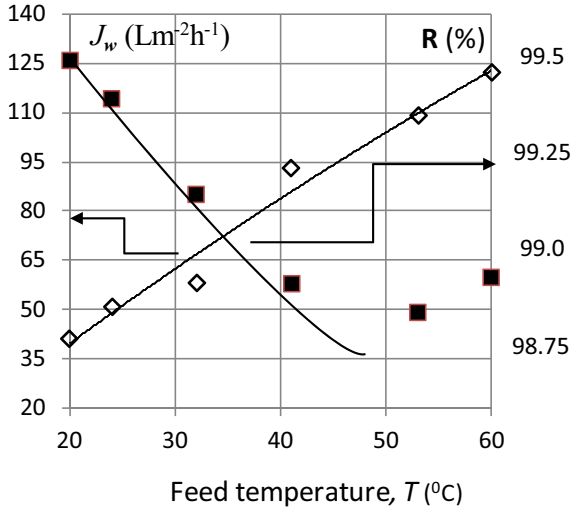

Fig. 1. Permeate flux J_w, and salt rejection R as the function of the feed temperature. NaCl concentration C_f = 3.5 m%, transmembrane pressure is 67 bar, T = 25°C. The symbols are the measured values [11,18].

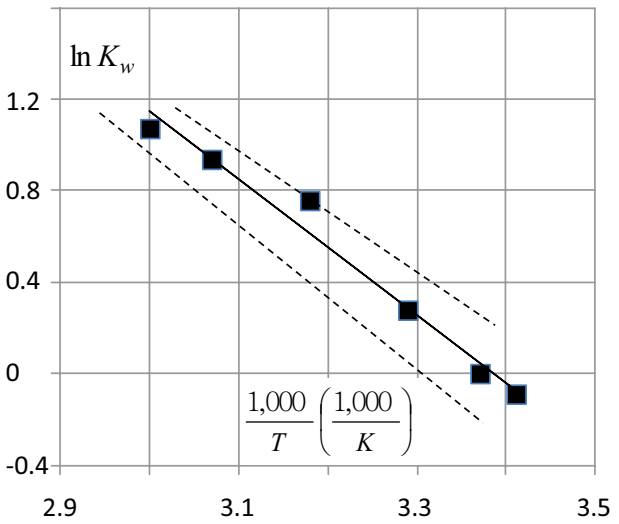

Fig. 2. Pre-exponential coefficient and activation energy associated with the water flux, from the data in Fig. 1, with the measured values (symbols) the fitted (dashed) and the limit (broken) curves.

Using Eq. (21) and considering the logarithm of both sides:

$$\ln K_s = \ln K_{s,0} - \frac{E_{a,s}}{R_g}\frac{1}{T} \tag{23}$$

where $E_{a,s}$ is the activation energy of the salt transfer process calculated from the slope, while its axial section is the logarithm of the pre-exponential coefficient.

3. Experiments and results

3.1. Experiments

For the controlling of the mass transfer model, the measurements of Al-Mutaz, Al Ghunaimi [11] and Cadotte et al. [18] have been used, where the permeate (water) flux ($J \cong J_w$) and salt rejection (R) were measured for sea water (NaCl) at a salt concentration of 3.5 m% as a function of the feed temperature (Fig. 1). The other parameters were: f_0 = 0.745, the transmembrane pressure, Δp = 67 bar, and αR_g = 0.0254 bar m%$^{-1}$ K^{-1} [17]. In this study, the J_w flux was measured in Lm^{-2} h^{-1} (2.78 × 10^{-7} m^3 m^{-2} s^{-1}), and the pressure in bar (10^{5}Pa). Accordingly, the dimension of the K_w mass transfer coefficient for water and the associated $K_{w,0}$ pre-exponential coefficient was Lm^{-2} h^{-1} bar^{-1}. The dimension of R is %, while that of the activation energies is kJ mol^{-1}.

3.2. Mathematical method

The temperature dependence characteristics of the transmembrane process based on Eqs. (20) and (23) were calculated by linear regression (EXCEL). The regression line:

$$y = a(x - x_0) + b. \tag{24}$$

Using the student test t_{n-2} [17–19], where n is the number of measurements, and $f = n - 2$ is the variability. The estimated values of the parameters are $\hat{a}$ and $\hat{b}$and that of Eq. (24) is $\hat{y}$ (point estimation). The 0-hypothesis is $\mathbf{H}_0$:$\hat{y} = y$, which is accepted at a 95% probability level, if $t_{n-2} > t_{f,0.95}$, where $t_{f,0.95}$ is the value belonging to the 95% (one-side) probability level (table of the student's test).

The standard errors of parameters s_a and s_b were calculated by the known formulas referred to in a parallel work in this volume [20]. Finally a confidence interval (both sides) of 95% has been determined for a $\left[\hat{a} - t_{f,0.975}s_a; \hat{a} + t_{f,0.975}s_a\right]$ and for b as well. P = 1 – 0.95 = 0.05 is the significance level [20] (interval estimation).

On the basis of the above-mentioned two limits, upper (+) and under (–), the correlation can be defined as follows:

$$\hat{y}^{\pm} = \hat{a}^{\pm}x + \hat{b}^{\pm} = (\hat{a} \pm t_{n-2,0.975}s_a)x \pm (\hat{b} \pm t_{n-2,0.975}s_b) \tag{25}$$

Using the confidence interval (both sides) of 95%. The area between two lines is where 95% of the measured points are placed.

3.3. Results

From Eq. (20) temperature dependence of the water mass transfer coefficient K_w, the values are: $y = \ln K_w$, $a = -\frac{E_{a,w}}{1,000R_g}$, $x = \frac{1,000}{T}$, $x_0 = 3$ and $b = \ln K_{w,0} - ax_0$. The estimated values and standard errors of the fitting parameters are: $\hat{a}$ = –2.97 K, s_a = 0.12 K, and $\hat{b}$ = 1.19 (unit) and s_b = 0.05 (unit); furthermore, R^2 = 0.9753, n = 6, f = 4, and from this, t_{n-2} = 12.6 > $t_{4,0.95}$ = 2.13 therefore the 0-hypothesis can be accepted. The confidence intervals of 95% ($t_{4,0.975}$ = 2.78) are [–3.30; –2.64] for a and [1.05; 1.33] for b.

Using $\hat{b}$ the estimated value of the pre-exponential coefficient is $\hat{K}$ = 24.3Lm^{-2} h^{-1} bar^{-1} (24.3 mh^{-1} bar^{-1}), and the activation energy of the process is $\hat{E}_{a,w} \cong 25$ kJ mol^{-1} with a 22–28 kJ mol^{-1} confidence interval. The diagram of the Eq. (20) water flux calculated with the parameters obtained as above as the function of the feed temperature, compared to the measurement results [11,19], and the limit curves of Eq. (25) belonging to a 95% probability level are shown in Fig. 2.

From Eq. (23) temperature dependence of the salt mass transfer coefficient K_s, the values are: $y = \ln K_s$, $a = -\frac{E_{a,s}}{1{,}000R_g}$, $x = \frac{1{,}000}{T}$, x_0 = 3, and $b = \ln K_{s,0} - ax_0$. The estimated values and standard errors of the fitting parameters are: $\hat{a}$ = –4.71 K, s_a = 0.62 K, and $\hat{b}$ = –0.73 (unit) and s_b = 0.17 (unit); furthermore, R^2 = 0.9321, n = 6, f = 4, and from this, t_{n-2} = 7.4 > $t_{4,0.95}$ = 2.13, therefore the 0-hypothesis can be accepted. The confidence intervals of 95% are [–6.43; –2.98] for a and [–1.20; –0.14] for b.

From $\hat{b}$ the estimated value of the pre-exponential coefficient is $\hat{K}_{s,0}$ = 6.6 ·10^5 Lm^{-2} h^{-1} bar^{-1} (660 m h^{-1} bar^{-1}) and the activation energy of the process is $\hat{E}_{a,s} \cong 39$ kJ mol^{-1} with a 25–53 kJ mol^{-1} confidence interval. The diagram of Eq. (20) water flux calculated with the parameters obtained as above as the function of the feed temperature, compared to the measurement results [11,19] furthermore, Eq. (25) limit curves belonging to the 95% probability level are shown in Fig. 3. In both cases the area between two lines shows where 95% of the measured values are placed.

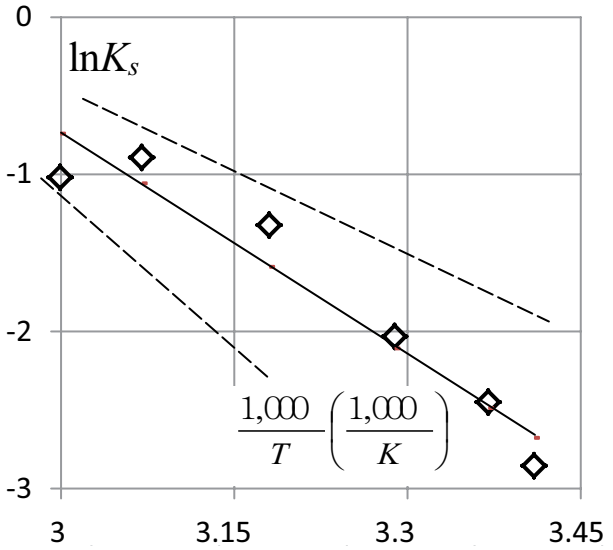

Fig. 3. Pre-exponential coefficient and activation energy associated with the salt flux, from the data in Fig. 1, with the measured values (symbols) the fitted (dashed) and the limit (broken) curves.

4. Discussion

The permeate (water) flux exhibits a J_w Arrhenius-type temperature dependence, where the pre-exponential coefficient is also slightly dependent on the temperature. The measured value of the activation energy $\hat{E}_{a,w} \cong 25$ kJ mol^{-1} (with a 22–28 kJ mol^{-1} confidence interval at a 95% probability level) is greater than that obtained for the process from the Poiseuille model, E_η = 16 kJ mol^{-1} value associated with the viscosity. The increased activation energy cannot be explained solely by the Poiseuille-law relating to the cross-membrane flow, since the viscosity causing the temperature dependence does not change to such an extent from a few % of dissolved salt that it could increase the energy to such a degree.

Viscosity is based on the friction between liquid layers (internal friction), which is caused by the force between molecules. If the pore size (diameter δ = 0.2 – 2 nm) is roughly the molecule size (diameter d_w = 0.2 nm in the case of H_2O), therefore the friction is determined by the force between the water molecule and the pore wall at first. As the latter is greater than the former, so the associated an (effective) activation energy, E^*_η must be also greater $E^*_\eta > E_\eta$. Finally, the activation energy of the process depends on the ratio of the molecules on surface and in volume, n_{surf}/n_{vol}, which is proportional to the quotient of the two sizes, $\frac{d}{\delta}$. Increasing this latter, the activation energy grows, further $E^*_\eta \to E_\eta$, if $\frac{d}{\delta} \to 0$. As $\frac{d}{\delta} > 0$, therefore $E_{a,w} = E^*_\eta > E_\eta$.

In the other hand, increasing the pole size, d, the activation energy of the water flux, $E_{a,w} = E^*_\eta$ decreases, that is, $E^*_\eta \to E_\eta$ if $d \to \infty$. It means that $E_{a,w}$ depends on the pore size (type) of the membrane. In accordance with this, from data obtained in a study on a completely different subject (germination process) [21] we achieved 19 kJ mol^{-1} for the water transfer across the membrane [19], which is also higher than for the greater viscosity but smaller than the mentioned value, since the pore size is also greater.

The salt transfer coefficient, K_s also exhibits an Arrhenius-type temperature dependence. The activation energy calculated from the measurements is $\hat{E}_{a,s} \cong 39$ kJ mol^{-1} with a 25–53 kJ mol^{-1} confidence interval. This interval is rather wide caused by the small change of the R value (98.85–99.5) in the measured temperature range. The activation energy of the salt flux, which is also greater than that associated with the water flux, $\hat{E}_{a,w}$ = 25 kJ mol^{-1}. As $d_s > d_w$ (d_s = 0.3 nm), therefore $\frac{d_s}{\delta} > \frac{d_w}{\delta}$, however, in accordance with the model, it follows that the activation energy of salt transfer process, $E_{a,s}$ will be greater than that of water flux, $E_{a,w}$.

As a consequence of the above, the water flux through the membrane is proportional to the applied pressure, while that of the salt is independent of it. This means the membrane will become more and more selective as the pressure increases.

Around 50°C, the salt rejection coefficient starts to diverge from the Arrhenius line, or even turns back. Since the permeate (water) flux is still an Arrhenius-type flux, the difference is only caused by the decrease in the salt flux, which can be caused by the decrease in activation energy. The reason for this can be that the higher temperature changes the structure of the membrane material – most often a composite membrane – and thus also the friction conditions.

5. Conclusion

The Arrhenius temperature dependence is suitable for describing the dependence of both the permeate flux, and the salt rejection coefficient on the feed temperature. By increasing the feed water temperature, the transmembrane pressure associated with the same flux decreases, that is, at a higher temperature a smaller pressure – smaller pump performance – is sufficient to take away the same quantity, which saves energy. Nevertheless, it is important to note that the permeate salt concentration increases with temperature, which must be taken into consideration in all cases, as well as the fact that the membrane material itself can also suffer at higher temperatures.

Acknowledgments

Project no. KFI_16-1-2017-0126 has been implemented with the support provided from the National Research, Development and Innovation Fund of Hungary, financed under the "KFI_16" funding scheme.

Symbols

C	—	Concentration, mol m^{-3}, m%
E	—	Energy, J, kJ
J	—	Flux, m^3 m^{-2} s^{-1} = ms^{-1}
K	—	Mass transfer coefficient, mPa^{-1} s^{-1}
K_α	—	Dissociation constant
R	—	Salt rejection factor, %
R_g	—	Gas constant, 8.314 J mol^{-1} K^{-1}
T	—	Temperature, K, °C
P	—	Probability level, %
a	—	Parameter, –
b	—	Parameter, –
d	—	Size (diameter) of molecule, m
f	—	Degree of freedom
f_0	—	Osmotic coefficient
n	—	Number of measurements
n	—	Number of pores
p	—	Pressure, Pa, bar
q	—	Rate, –
t_f	—	Student test

Greek

β	—	Temperature constant, K
ν	—	Dissociation number
π	—	Osmotic pressure, Pa, bar
δ	—	Size (diameter) of pore, m
ε	—	Porosity
λ	—	Length, m
η	—	Viscosity, m^2 s^{-1}
ρ	—	Density, kg m^{-3}

Indexes

^	—	Estimated value
$_0$	—	Initial value
$_0$	—	Pre-exponential
$_a$	—	Activation
$_f$	—	Feed
$_p$	—	Permeate
$_s$	—	Salt
$_w$	—	Water value
$_-$	—	Back

References

[1] K. Jeong, M. Park, T.H. Chong, Numerical model-based analysis of energy-efficient reverse osmosis (EERO) process: performance simulation and optimization, Desalination, 453 (2019) 10–21.
[2] A.E. Anqi, N. Alkhamis, A. Oztekin, Steady three dimensional flow and mass transfer analyses for brackish water desalination by reverse osmosis membranes, Int. J. Heat Mass Transfer, 101 (2016) 399–411.
[3] B. Bernales, P. Haldenwang, P. Guichardon, N. Ibaseta, Prandtl model for concentration polarization and osmotic counter-effects in a 2-D membrane channel, Desalination, 404 (2017) 341–359.
[4] K. Bélafi-Bakó, Membrane Operations, Veszprémi Egyetemi Kiadó, Veszprém, 2002.
[5] L.-Y. Hung, J.L. Shingjiang, J.-H. You, Mass-transfer modeling of reverse-osmosis performance on 0.5–2% salty water, Desalination, 265 (2011) 67–73.
[6] M. Mulder, Basic Principles of Membrane Technology, Kluwer Academic Publishers, Dordrecht, 1996.
[7] M. Pontié, H. Dach, J. Leparc, M. Hafsi, A. Lhassani, Novel approach combining physico-chemical characterizations and mass transfer modelling of nanofiltration and low pressure reverse osmosis membranes for brackish water desalination intensification, Desalination, 221 (2008) 174–191.
[8] M.A. Ebrahim, S. Karan, A.G. Livingston, On the influence of salt concentration on the transport properties of reverse osmosis membranes in high pressure and high recovery desalination, J. Membr. Sci., 594 (2019) 117339.
[9] M. Li, Predictive modelling of a commercial spiral wound seawater reverse osmosis module, Chem. Eng. Res. Des., 148 (2019) 440–450.
[10] A. Ruiz-García, I. Nuez, Long-term performance decline in a brackish water reverse osmosis desalination plant. Predictive model for the water permeability coefficient, Desalination, 397 (2016) 101–107.
[11] I.S. Al-Mutaz, M.A. Al-Ghunaimi, Performance of Reverse Osmosis Units at High Temperatures, The IDA World Congress on Desalination and Water Reuse, Bahrain, 2001.
[12] J. Lakner, G. Lakner, P. Bakonyi, K. Belafi-Bako, Temperature dependence of transmembrane-chemi-sorption for waste water with ammonia contents, Desal. Water Treat., (2020), doi: 10.5004/dwt.2020.25962.
[13] W.B. Baker, Membrane Technology and Applications, A John John Wiley & Sons, Chichester (UK), 2012.
[14] T. Tse-Pei, Hole theory of the liquid state, Nature, 157 (1946) 873–874.
[15] Engineering ToolBox, Water - Dynamic and Kinematic Viscosity, 2004. Available at: https://www.engineeringtoolbox.com/water-dynamic-kinematic-viscosity-d_596.html
[16] T. Erdey Grúz, Fundamentals of Physical-Chemistry, Műszaki Könyvkiadó, Budapest, 1972.
[17] J. Lakner, G. Lakner, G. Racz, Concentration dependence modelling of reverse osmosis, Desal. Water Treat., (2020), doi: 10.5004/dwt.2020.25906.
[18] J.E. Cadotte, R.J. Petersen, R.E. Larson, E.E. Erickson, A New Thin Film Sea Water Reverse Osmosis Membrane, Presented at the 5th Seminar on Membrane Separation Technology, Clemson University, Clemson, SC, 1980.
[19] G. Lakner, J. Lakner, Mathematical modeling for stages in germination of common reed (*Phragmites australis*), Acta Bot. Hung., 52 (2010) 341–361.
[20] G. Lakner, J. Lakner, P. Bakonyi, K. Belafi-Bako, Kinetics of transmembrane chemisorption for waste water with high ammonia contents, Desal. Water Treat., (2020), doi: 10.5004/dwt.2020.25872.
[21] A.M. Mayer, A. Poljakoff-Mayber, The Germination of Seeds, 3rd ed., Pergamon Press, London, 1982, pp. 37–43.